Remote Sensing at the Service of Wetlands Mapping: A Case of the Lower Loukkos Complex (North-West Morocco)

Badreddine Fathi[1*], Abdelghani Afailal Tribak[1], Miriam Wahbi[2],
Mustapha Maâtouk[2], Boutaina Sebbah[2]

[1] Research Team on Natural Risks, Faculty of Sciences and Techniques, Tangier, Abdelmalik Essaadi University, Tetouan, BP 416, Morocco
[2] Research Team in Geomatics Remote Sensing and Cartography, Faculty of Sciences and Techniques, Tangier, Abdelmalik Essaadi University, Tetouan, BP 416, Morocco
* Corresponding author's e-mail: badreddine.fathi@etu.uae.ac.ma

ABSTRACT

Despite their highly recognized ecological values and ecosystem services, approved by the scientific community, wetlands are in perpetual degradation and their global spatial extension in significant regression. The conservation and sustainability of such ecosystems begins with their monitoring and delimitation. This study aims to develop an approach using open access remote sensing data to make this delineation. Applied to the coastal wetland complex of the lower Loukkos in the Mediterranean area, the methodology followed a two-step process. Firstly, it predicted the spaces favourable for water accumulation conditions, and secondly, it identified the presence of water and its response on the soil and vegetation. The approach was based on a theoretical modelling adopting the potential, existing, efficient wetland (PEEW) approach. The recordings from Sentinel sensors served as the basis for calculating indices Beven-Kirkby Index (BKI), Buffer zone Index (BZI), Normalized Difference Moisture Index (NDMI), Normalized Difference Vegetation Index (NDVI) and Modified Normalized water difference index (MNDWI) to pre-locate and model potential wetland areas (PW). Photointerpretation was used to map the existing wetland areas (EW). The estimated area of wetlands in the lower Loukkos region is 379 km² for potential areas identified from topographic data and the hydrographic network, 120 km² for areas dominated by wetlands detected by remote sensing of water bodies , vegetation and soil moisture, and 33 km² for natural wetlands identified by photo-interpretation. As a result, the area of current wetlands is only about 9.5% of their theoretical past extent. The validity of this method was confirmed through a comparison of the results with field investigations and hydromorphic traits in soil surveys, as well as external soil mapping data, showing an 84% concordance.

Keywords: wetlands, delimitation, remote sensing, cartography, GIS.

INTRODUCTION

With only 2.6% of land area, wetlands are the primary producer of organic matter, the largest biodiversity hotspot globally (Skiner and Szalewski, 1995). Their ecological benefits surpass those of other ecosystems. However, wetlands have been experiencing a gradual decline that has accelerated in recent decades, with a loss of approximately 35% of their extent between 1970 and 2015 (Ramsar Convention, 2018). Despite awareness of this massive disappearance in recent decades and the multitude of conservation initiatives, wetlands continue to degrade degrade (Acreman et Mccartney, 2009; Beltrame et al., 2015), with 35% of global wetlands at risk of disappearing at an annual disappearance rate between 0.85% and 1.6% (Gardner and Finlayson, 2018). Given this observation, the detection, delimitation, and monitoring of wetland changes have become essential for their conservation. Currently, 2431 sites are recognized as internationally important under the Ramsar Convention. However, small wetlands with ordinary biodiversity are still not adequately

inventoried (Merot et al., 2006). Wetland delimitation faces several conceptual difficulties due to the plurality of their definitions, the diversity of their nature, and the intra- and interannual fluctuations of their boundaries related to water quantity in these environments. Methodological challenges also arise due to their often extensive size, typically covering areas of square kilometers, as well as limited access to frequently flooded areas and their gradually transitioning boundaries. In response to these challenges, remote sensing has long been recognized as an effective tool for wetland mapping (Cowardin and Myers, 1974; Rapinel et al., 2019). The technological progress of satellite imagery and the popularization of its promising products contribute to overcoming certain difficulties in extracting credible information for the determination of components with a humid character. these components are essential for mapping wetlands. The potential of satellite data has greatly evolved to detect surface water bodies, soil hydromorphy and hygrophylous vegetation which are the basis for the identification and delimitation of wetlands.

This work aims to develop a reliable approach for the discrimination of the characteristic components of wetlands in order to identify and delimit these ecosystems at site level. It also aims to investigate the potential of freely accessible high-resolution satellite images for mapping the extent of surface water and the response of prolonged water presence on the soil and vegetation.

WETLANDS DELIMITATION PROBLEMATIC

Wetlands delimitation challenges

The delimitation of wetlands refers to determining the boundaries between wetland and non-wetland areas. These boundaries often have gradual transitions without clear spatial and temporal borders with adjacent ecosystems (Yarrow et al., 2008), The delimitation process is primarily based on the definition of wetlands, which can vary depending on the objectives of scientists, policymakers, or managers. Delimitation can rely on direct criteria related to the presence of water, such as flood level fluctuations, groundwater table variations, or tidal fluctuations. However, due to the seasonal and annual fluctuations of water masses within these ecosystems, delimitation

mostly relies on indirect criteria. These include the response of the soil morphology to prolonged water presence, particularly related to iron form (MEDDE, GIS Sol. 2013), as well as the distribution of vegetation and wildlife (Decree n°2007–135 of 30 January 2007) (Bouzille et al., 2014). The specificity of the discrimination criteria, which vary across different definitions, the most famous of which are those of the Ramsar Convention in 1971, of the International Biological Program of the United Nations Educational, Scientific and Cultural Organization (UNESCO) in 1974. This plurality of definitions influences the level of restriction in the delimitation.

The diversity of wetland environments shapes the delimitation methodologies, which adapt to the size and nature of the wetland. Wetlands often cover large areas, and fieldwork to delimit them is time-consuming and requires expert personnel. This is why remote sensing is widely used in most studies. Additionally, the spatial monitoring of wetlands requires repetitive measurements, which are facilitated by the temporal resolution of satellite sensors.

Delimitation methods

The methodologies for delimiting wetlands are diverse and adapt to the nature of the specific wetland ecosystem, as well as the criteria considered for delimitation. We can distinguish between indirect modelling methods, known as theoretical methods, and direct field-based delimitation methods. Indirect modelling methods involve using remote sensing data and geographic information systems (GIS) to assess various indicators and parameters associated with wetland characteristics. These methods often rely on the analysis of satellite imagery and the extraction of specific features or signatures related to wetland presence, such as water indices, vegetation indices, or soil characteristics. These modelling approaches provide valuable information for identifying potential wetland areas and predicting their spatial distribution.

On the other hand, direct field-based delimitation methods involve physically visiting the wetland sites and collecting on-site data to determine the boundaries. This can include surveying the water levels, soil properties, vegetation composition, and other relevant parameters that help define the wetland boundaries. Field observations and measurements are essential for verifying the

presence of wetland characteristics and refining the delimitation based on ground truth information. The choice of delimitation method depends on factors such as the scale and size of the wetland, the available resources, and the specific objectives of the study. Often, a combination of remote sensing techniques and field-based verification is employed to achieve more accurate and reliable wetland delimitation results.

Theoretical modelling methods primarily rely on cartographic and remote sensing surface data, which continue to advance in terms of spatial, spectral, and temporal resolution. These methods utilize data on pedology, habitats, and vegetation. Optical Very High-Resolution Satellite Imagery (VHRS) is used to map hydromorphic soils (Bailly et al., 2003). Surface and subsurface soil moisture can also be revealed using spectral bands in the thermal infrared (IRT) (Bendjoudi & Hubert, 2002; Brahmi et al., 2010) and the mid-infrared (MIR) if atmospheric conditions permit (Escadafal et al., 1993), or by combining optical and RADAR images (Elhajj and al., 2018). Hygrophilous vegetation serves as an indirect indicator of soil moisture and fertility (Ellenberg et al., 1991). The precision of characterizing this indicator depends on the type of remote sensing data used, each of which presents obstacles to overcome. These obstacles include limited spatial coverage for aerial photographs, coarse identification of often heterogeneous vegetation formations in wetland areas for Very High-Resolution Satellite optical images (VHRS), difficulties in vertical discrimination for VHRS Imagery, and the sensitivity of fine-resolution RADAR images to both canopy roughness and moisture (Bouzilé, 2014). Light Detection And Ranging (LiDAR) data can provide detailed information on canopy structure (Rapinel, 2012), but they do not allow for discrimination between different habitats. The combination of different types of remote sensing data appears to be most suitable for wetland vegetation mapping (Gilmore et al., 2008). Sentinel-1 RADAR and Sentinel-2 optical images offer new perspectives for delimiting these ecosystems. The spectral bands 5, 6, and 7 of Sentinel-2 optical images, with a spatial resolution of 20m, are specifically designed for vegetation and allow for the creation of vegetation maps with good spatial resolution (Corbane et al., 2015). The various vegetation structures can be differentiated thanks to the spectral resolution of these sensors (Dusseux, 2014).

For image processing, two approaches can be considered: analog image interpretation and digital processing through pixel-based or object-based analysis. The hybrid approach, which combines both methods, is the most common as it optimizes cost, time, and personnel while achieving satisfactory accuracy in wetland delineation.

Field data is used to validate the theoretically calculated models. Field-based methods rely on the collection, recording, interpolation, and spatialization of in-situ information obtained through point sampling of flood duration, groundwater level, and the presence of hygrophytic vegetation. Examples include studies by Cazals et al. (2016) on soil hydromorphy (as defined by the Association of Exporters and Professionals of Agricultural Products GEPPA, a study group on applied pedology problems, in 1981; modified) or the dominance of hygrophytes listed in the amended decree of June 24, 2008, as studied by Davranche (2008).

Sampling points are collected along transects perpendicular to the assumed boundary between the wetland and non-wetland areas, identified by flood levels, groundwater levels, or tidal influence. The distribution of sampling points should account for the heterogeneity of the terrain, typically with one sample taken per hydrogeomorphological unit.

MATERIALS AND METHODS

Study area

To study the contribution of satellite imagery in delineating wetland areas, we conducted our study in the Lower Loukkos complex shown in Figure 1, located near Larache in northern Morocco at the mouth of the Loukkos River (35°07'N 06°00'W). This complex was designated as a Ramsar Site of Biological and Ecological Interest and an Important Bird Conservation Area in 2005. Covering an area of 3600 hectares, the complex encompasses a portion of the lower Loukkos valley, including its tributaries, marshes, and salt marshes.

The climate in this region is Mediterranean, with an oceanic influence, characterized by average annual precipitation of 779 mm and an average annual temperature of 17.9°C. The hydrology of the area is influenced by the water inputs from the Loukkos River, estuarine waters, runoff, the Lower Loukkos aquifer, and irrigation water (Dakki, 2002).
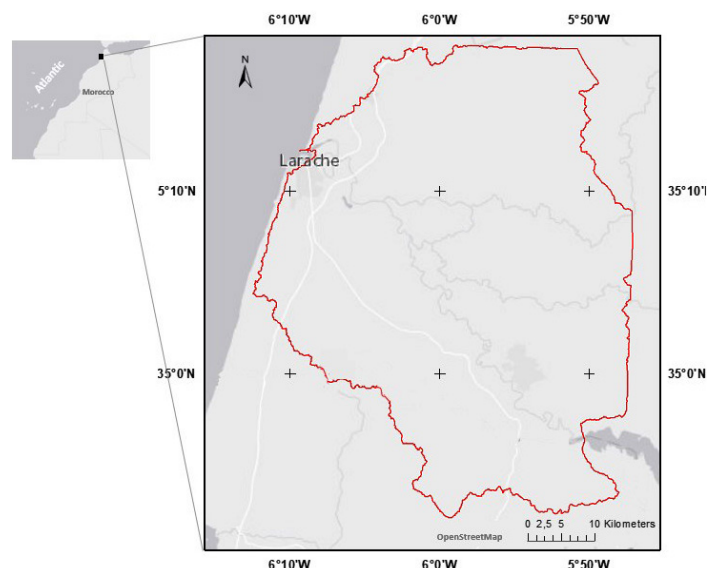
Figure 1. Map showing the study area in the complex of the lower Loukkos wetlands

The delimitation method

The delimitation of the lower Loukkos complex is based on the Potential Existing Efficient Wetlands (PEEW) approach, which utilizes available cartographic data, maps derived from remote sensing data, and field investigations. The different layers of information used to map the wetlands of the lower Loukkos complex are shown in Table 1. This delineation process involves identifying Potential Wetlands (PW) and then delineating Existing Wetlands (EW) as shown in Figure 2.

Calculation of potential wetland areas

Delimitation of potential wetlands (PW) areas – the geomorphology and climate determine the characteristics of an area within a watershed to acquire the features of a wetland. The Beven-Kirkby Index (BKI) is an estimation index for potentially hydromorphic soils that may be saturated with water permanently or temporarily (Beven

and Kirkby, 1979). To define the boundaries of the envelope where the probability of water accumulation is high enough to generate hydromorphic conditions and establish wetland areas, our methodological approach follows four steps. Estimation of the topographic hydromorphy model, Calculation of the buffer zone around the hydrographic network, Remote sensing estimation of areas with wetland dominance, and spatial analysis to combine these three envelopes.

Estimation of the hydromorphic model: To pre-locate wetlands in the study area, the downstream BKI index was calculated, which provides more relevant results than the traditional BKI index (Aurousseau and Squividant, 1995), using a Geographic Information System (GIS) and the Digital Elevation Model (DEM). Two altitude thresholds delineating three hydromorphological envelopes with low, medium, and high probability of existence were estimated based on soil verification on the pedological map at test sites. The spatial analysis that

Table 1. The characteristics of the data used during the delimitation of the lower Loukkos complex.

Layer	Format	Date	Resolution / scale	Source
DEM	Raster	2021	12.5 m	NASA – National Aeronautics and Space Administration
Soil map	Raster	1950	1/5000	TEMA/ORMVAL – Regional Office for Agricultural Development of Loukkos
Optical sentinel image	Raster	2022	10 m	ESA – European Space Agency
Satellite image	Raster	2022	1 m	Maxar Technologies /Google
Surface water recurrence map	Raster	2021	10 m	EC JRC/Google – European Commission's Joint Research Centre, UN Environment
Soil soundings	Vector	2022	–	Field trip
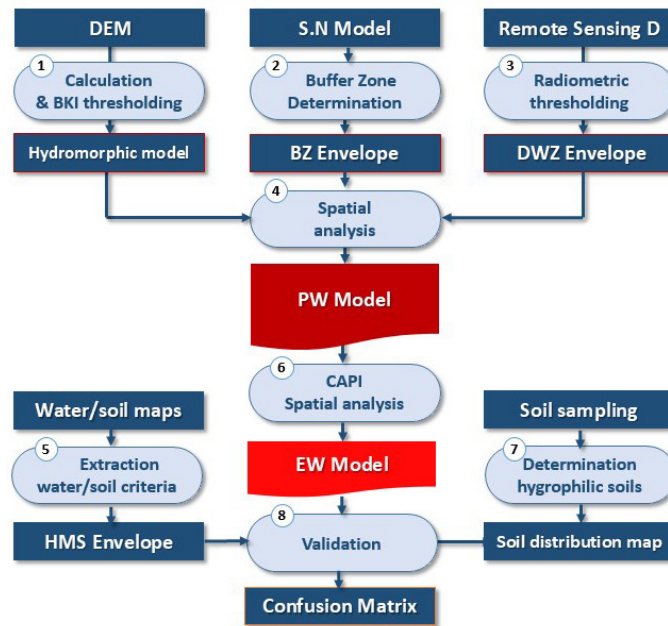
Figure 2. Methodological diagram for wetland delimitation in the Lower Loukkos area

combines these results allowed the mapping of these three envelopes.

Calculation of the hydrographic network buffer: The hydrographic network and water bodies were extracted from the digital elevation model and corrected using Sentinel images. The determination of Buffer Zones (BZ1) around the linear hydrographic network and (BZ2) the surface hydrographic network is based on iterative calculation under GIS, at each point, of the distance from the nearest watercourse or water body up to a threshold. This threshold takes into account the branch order of the watercourse for BZ1 and the area of the water body for BZ2. The boundaries of non-perched wetland areas depend mainly on the topography on the lateral axis of the hydrographic network (Rapinel, 2012). Therefore, a change in the reference level of altitudes that considers the level of the watercourse bed is necessary as

illustrated in Figure 3. Using the Digital Elevation Model (DEM) normalized to the sea level, the normalized digital watercourse model (NDWM) was calculated with respect to the watercourse bed within the buffer zone around the hydrographic network, in order to establish the altitude thresholding.

The iterative segmentation under GIS using the "Contrast Split" algorithm of the NDWM layer into contour lines with a 1m equidistance allows for the refinement of the buffer zone around the hydrographic network. The altitude limit of the buffer zone around watercourses was determined based on the map of hydromorphic soils. Figure 4 shows the procedure for calculating the Cross-Index (CI) of the probability of wetland presence, using the results of the theoretical modelling on the two criteria, the topographic index (BKI) and the buffer zone index (BZI), this
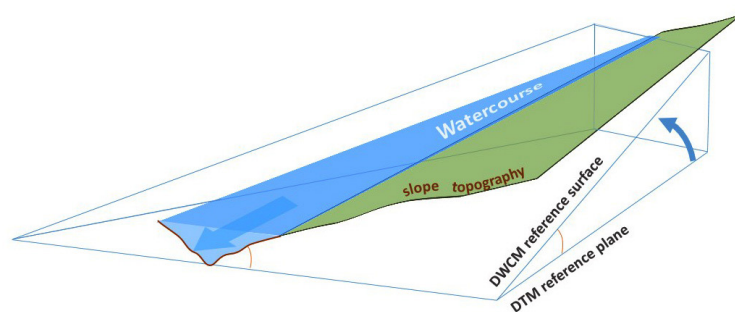
Figure 3. Diagram illustrating the conversion of the reference plane to calculate the normalized digital watercourse model (NDWM)

allows for a more precise delineation of potential wetland areas.

Estimation of wetland-dominated areas: Using remote sensing Water, hygrophilous vegetation, and hydromorphic soil are the three components included in most wetland definitions, including the Ramsar Convention definition. The operational approach used in this study, presented in the diagram in Figure 5, involves thematic extraction to determine three entities: "surface water," "marsh vegetation," and "hydromorphic soil." These entities form the components of the Wetland-Dominated Area (WDA) envelope. Spectral thresholding is applied to three newly created indices, Normalized Differential Moisture Index (NDMI), Normalized Difference Vegetation Index (NDVI), and Modified Normalized Water Difference Index (MNDWI), which are calculated from the Sentinel image, to determine these three entities.

The determination of the "hydromorphic soil" mask: The Normalized Difference Moisture Index (NDMI) is first used to assess the water content of vegetation (Gao, 1996), which also reflects
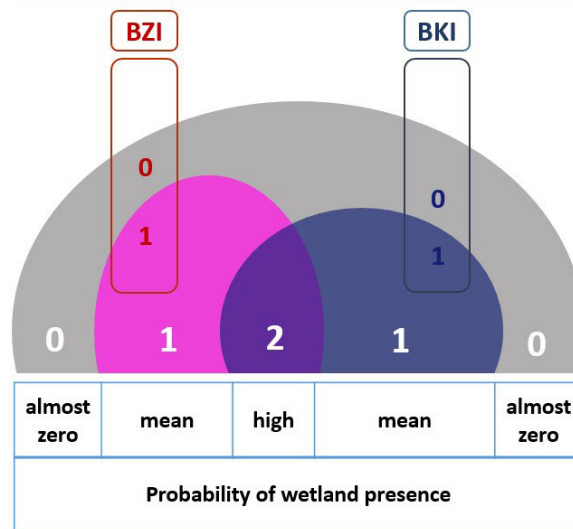
Figure 4. Diagram illustrating the calculation of the probability index of wetland presence resulting from the intersection of the topographic index (BKI) and the buffer zone index (BZI)
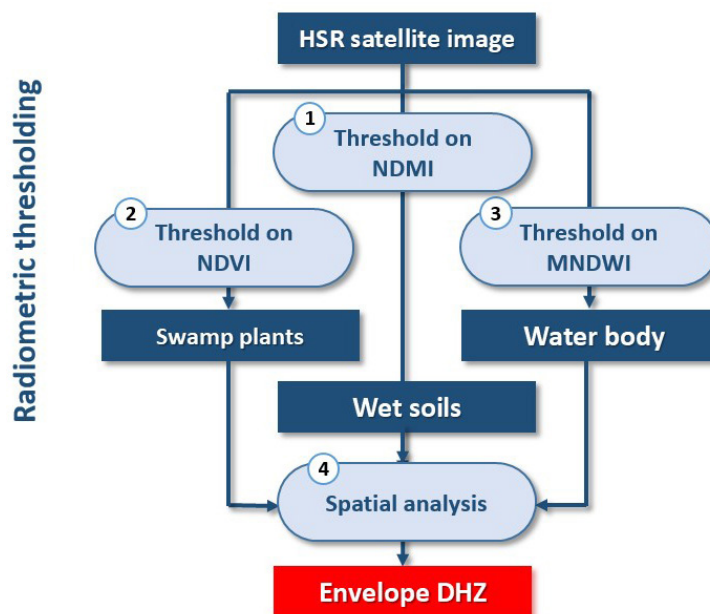
Figure 5. Methodological diagram for calculating the wetland-dominated area (WDA) in the Lower Loukkos complex

soil moisture. NDMI values range from -1 (water stress) to 1 (waterlogged).

$$NDMI = (NIR-SWIR) / (NIR+SWIR)$$

$$\text{For Sentinel 2:}$$
$$NDMI= (B8 - B11) / (B8 + B11) \tag{1}$$

Spectral thresholding on the NDMI channel allows for the extraction of the "hydromorphic soil" mask.

Extraction of wetland vegetation: The extraction of the "wetland vegetation" mask is based on the difference in activity between vegetation in wet and non-wet environments (shift in vegetation cycles) at the beginning of the dry season in summer. Radiometric thresholding on the NDVI layer, where positive values close to 1 indicate high water content, allows for the determination of the "wetland vegetation" mask.

$$NDVI = (NIR - RED) / (NIR + RED)$$

$$\text{For sentinel 2:}$$
$$NDVI = (B08 - B04) / (B08 + B04) \tag{2}$$

Determination of the "surface water" mask: The Normalized Difference Water Index (NDWI), primarily designed for vegetation water content detection (Gao, 1996), was modified by S.K. McFeeters (MNDWI) to detect surface water bodies. This index uses the green (G) and shortwave infrared (SWIR) wavelengths (MC Feeters, 1996):

$$MNDWI = (G - SWIR') / (G + SWIR')$$

$$\text{For sentinel 2:}$$
$$MNDWI = (B03 - B11) / (B03 + B011) \tag{3}$$

The two bands used to calculate MNDWI (G and SWIR) have different spatial resolutions of 10m and 20m, respectively, necessitating the improvement of the spatial resolution of the SWIR band (band 11). The pan-sharpening method, which merges the image to be enhanced with the panchromatic image, is commonly used (Vivone, 2015). Since the Sentinel-2 optical image does not have a panchromatic band, Y. Du (2016) used the 10m resolution bands to increase the spatial resolution of the SWIR band (band 11) and obtained relevant results during mNDWI calculation and the extraction of flooded surfaces using Sentinel multispectral scenes.

The calculation of the mNDWI channel using the fused band from band 2 and 11, followed by spectral thresholding, allows for the creation of the "surface water" surface mask. The OTSU algorithm was used to determine the threshold value t, as defined by (Otsu, 1979), which segments the MNDWI image into water and non-water classes based on the value of t. The optimal threshold value t∗ in the OTSU algorithm is determined as follows:

$$\delta^2 = P_{nw} \cdot (M_{nw} - M)^2 + P_w \cdot (M_w - M)^2 \tag{4}$$

$$M = P_{nw} \cdot M_{nw} + P_w \cdot M_w \tag{5}$$

$$P_{nw} + P_w = 1 \tag{6}$$

$$t^* = \text{Arg Max}$$
$$\{P_{nw} \cdot (M_{nw} - M)2 + P_w \cdot (M_w - M)^2\} \tag{7}$$

where δ: the interclass variance of the non-water class and the water class
Pw: probability of a pixel to belong to the water class
Pnw: probability of a pixel to belong to the non-water class
Mw: average value of the water class
Mnw: average value of the non-water class
M: average value of the MNDWI image.

The envelope of areas dominated by wetlands was delimited based on the combination of the three masks: "hydromorphic soil," "wetland vegetation," and "surface water."

Data combination: After the spectral thematic extraction of the three layers, including hydromorphic soils after thresholding on the BKI, the buffer zone of the hydrographic network, and the areas dominated by wetlands from spectral thresholding, the union of these three layers allows for the calculation of the model for potential wetland areas (PW).

Delimitation of existing wetlands

Effective wetland areas are encompassed within the envelope of potential wetland areas. However, these areas may partially lose their wetland characteristics due to natural or often anthropogenic causes, characterized by

hygrophilous vegetation and/or hydromorphic soil (Merot and al., 2006). The delimitation of effective wetland areas in the lower Loukkos region involves confirming the presence of wetland areas on the potential wetland map by verifying their wetland nature using pedological criteria. The hydromorphic nature of the soil, as a response to permanent or prolonged waterlogging, is a sufficient criterion for validation. The determination of the envelope of exesting wetlands (EW) was carried out in four steps, then validated by the confusion matrix. This diagram is shown in Figure 6.

Existing wetland mapping – within the ZHP, the effective wetlands are identified based on hydromorphic soils and hygrophilous vegetation. Photointerpretation of the extract from the Maxar scene, provided by Google Earth at a spatial resolution of 1m, on the envelope of ZHP allows for their mapping. This cartographic delineation meets the criteria set by the decree defining wetland areas.

Validation of the existing wetlands map – existing wetlands model is validated through ground truthing. The wetland nature of the calculated EW model is validated using exogenous cartographic data and field data. The overlay of this model is first compared with two types of exogenous data: the spatial distribution of hydromorphic soils and areas prone to flooding. Hydromorphic soils are extracted from pedological maps at a scale of 1/5000 provided by the TEMA company for Regional Office for Agricultural Development of Loukkos (ORMVAL), and areas with high recurrence of flooding are obtained from surface water distribution monitoring maps for the period 1984–2021 (at

a spatial resolution of 10m provided by the European Commission's Joint Research Centre (EC-JRC), Union Nations Environment (UN-E) and Google. Additionally, soil surveys (located by GPS near the model's boundary at control points) are conducted.

In the second phase, the EW model is validated through pedological tests performed in six marshes in the lower Loukkos region and in the buffer zone of the hydrographic network. the distribution of sampling stations is shown on the map in Figure 7. The presence of hydromorphic features in the soil samples is examined to assess the quality of the EW delineation.

To assess the accuracy of the modeling, the results of the spatial distribution mapping of EW were compared with three layers of information. These included hydromorphic soils derived from soil maps, areas with high recurrence of flooding obtained through remote sensing monitoring of surface waters over the past 3.8 decades from the cooperation between the Joint Research Centre of the European Commission, United Nations (UN) Environment, and Google, and the point characterization of soils through field sampling. The Kappa index is calculated using the following formula:

$$Kappa = (Po - Pc)/(Pp - Pc) \qquad (8)$$

where: *Po* is the observed correct proportion,
Pc the expected correct proportion due to chance
Pp the correct proportion when the classification is perfect.
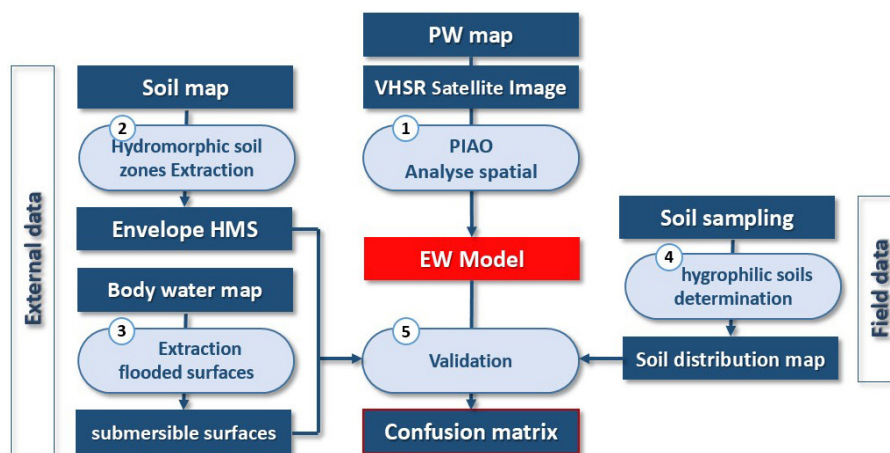
Figure 6. Methodological diagram for delimiting effective wetland areas in the lower Loukkos region
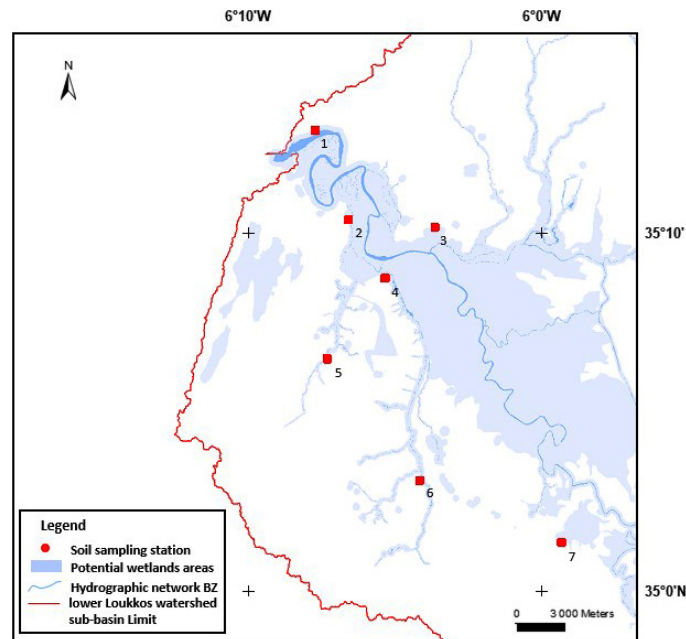
Figure 7. Map showing the location of pedological surveys in the three sampling stations within the study area

RESULTS AND DISCUSSION

Delimitation of potential wetlands

The topographic determination of hydromorphic zones.

The calculation of the BKI index based on the digital terrain model provided a topographic moisture index that ranged from 2.53 as the lowest value to 25.36 in areas with high water accumulation capacity, shown in green and blue on the Figure 8. These areas were primarily located in the alluvial plain and surrounded the drainage channels.

The comparison of the calculated BKI values with the soil nature at control points derived from the 1/5000 scale soil map revealed the hydromorphic conditions at these points and determined threshold values for IBK: 12.2, 11.57, and 10.76, which delineate three envelopes representing high, medium, and low probabilities of being hydromorphic soil areas. Extrapolating these results to the entire study area allowed for the calculation of a variable-sized hydromorphic model. After eliminating areas smaller than 0.3 hectares, the estimated surface area was 11.24 km², 19.8 km², and 62.79 km² for the high, medium, and low probability envelopes, respectively. The contour encompassing the high probability envelope delineates a total area of 270.26 km².

The calculated topographic hydromorphic model includes areas where surface drainage promotes water accumulation while excluding areas with low contributing area or steep slopes such as hills. However, errors were observed due to the accuracy of the digital terrain model. Refinement of the contour was performed by comparing this model with the soil map and topographic map.

The delimitation of buffer zones for the hydrographic network

The delimitation of the PW is mainly occurs on the lateral side of the river network, as observed in the BKI hydromorphic model, which generally surrounds linear ditches of watercourses and depressions of water bodies. The calculation of the buffer zone for the river network considered two criteria: distance and altitude from the hydrographic network. The Digital WaterCourse Model (DWCM) allowed for the altitude thresholding of the BZ envelope. The delineation thresholds, which vary according to the stream order and the surface area of water bodies, were calibrated based on the lateral extent of hydromorphic soils extracted from the soil maps on both sides of the control points on the river network. The results obtained are shown in Table 2 and the map in Figure 9.

The remote sensing of PW, based on the results obtained from the calculation of the BKI and BZI, enabled the mapping of wetland areas with a total area of 379 km² shown in Figure 10. This represents nearly 10.5 times the surface area of
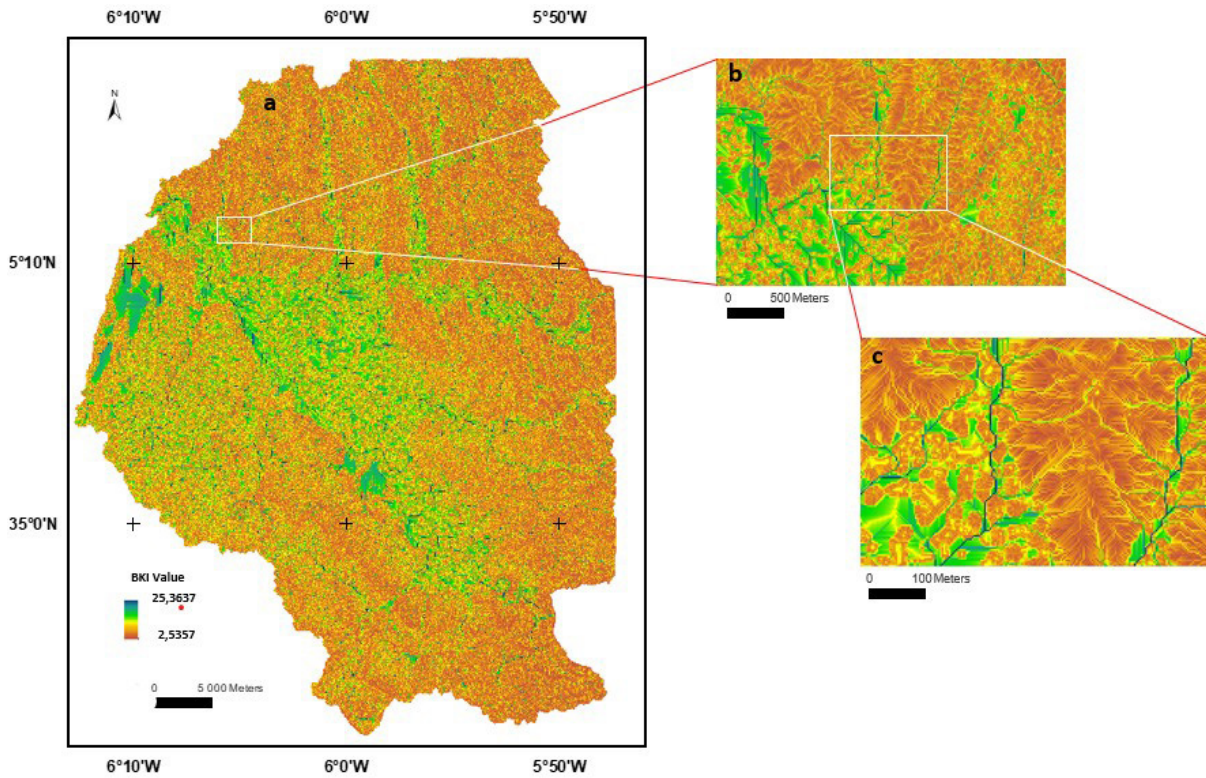
Figure 8. Beven-Kirkby index map calculated from a Digital Elevation Model in the Lower Loukkos Basin at different scales. (a) in the Loukkos sub-watershed, (b and c) detailed view of the alluvial plain boundary on the right bank of the Loukkos river

Table 2. Thresholds derived from control points for calculating the buffer zone of the hydrographic network in the Lower Loukkos Basin

Thresholds in relation to the hydrographic network	Stream order				Area of water bodies		
	1	2	3	4	40 < S < 400	400 < S < 1000	S <1000
Distance thresholds in "m"	50	100	150	250	50	100	150
Altitude thresholds in "m"	1	1	1	2	1	1	2
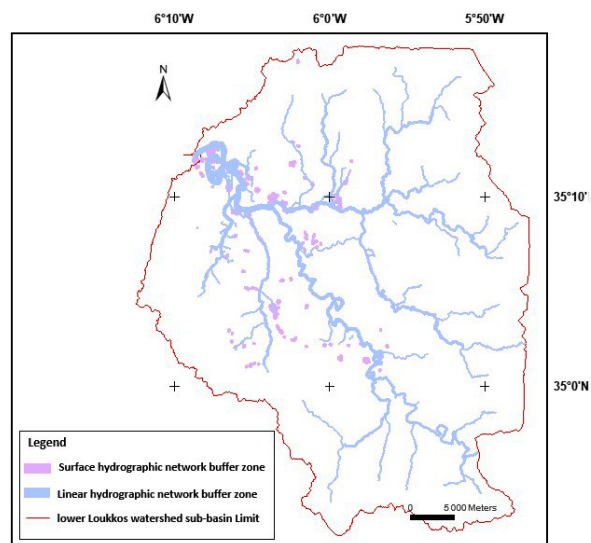
Figure 9. Buffer zone envelopes around the linear and surface hydrographic network in the Lower Loukkos Basin calculated through thresholding based on distance and altitude using a Digital Elevation Model

the wetlands in the Lower Loukkos Basin, which is 36 km² according to the Ramsar Convention (PDAP, 1994). The observed difference is mainly attributed to the gradual conversion of wetland parcels for agricultural activities and local development. Additionally, wetland areas with a diameter smaller than 10 m² were not mapped due to the resolution of the Digital Elevation Model (DEM). Some over-detections were also noted, resulting from considering the canopy top points as ground points in forested areas. To correct for over-detection and account for the limitations of the BKI and BZI indices in mapping PW, the use of Sentinel images highlighted the current state of the Lower Loukkos Basin.

Estimation of wetland-dominated areas through remote sensing: The delineation of these areas was based on three envelopes presented in Figure 11. The first envelope corresponds to surface water bodies, mainly influenced by meteorological variations. The second envelope represents "marshy vegetation" and the third envelope represents soil moisture. These last two envelopes indicate the prolonged presence of water on the ground.

Based on photointerpretation of Google Earth scenes, three thresholds for neo-channels were defined. The threshold values range from 0.6 to 0.98 for the Normalized Difference Moisture Index (NDMI), from 0.21 to 0.32 for the Normalized Difference Vegetation Index (NDVI), and from -0.99 to -0.74 for the modified Normalized Difference Water Index (MND-WI). Spectral thresholding on NDMI classified an area of 4 370 hectares as wetland soils. An envelope with an area of 1 258 hectares was classified as marshy vegetation based on thresholding on NDVI. The area of free surface water
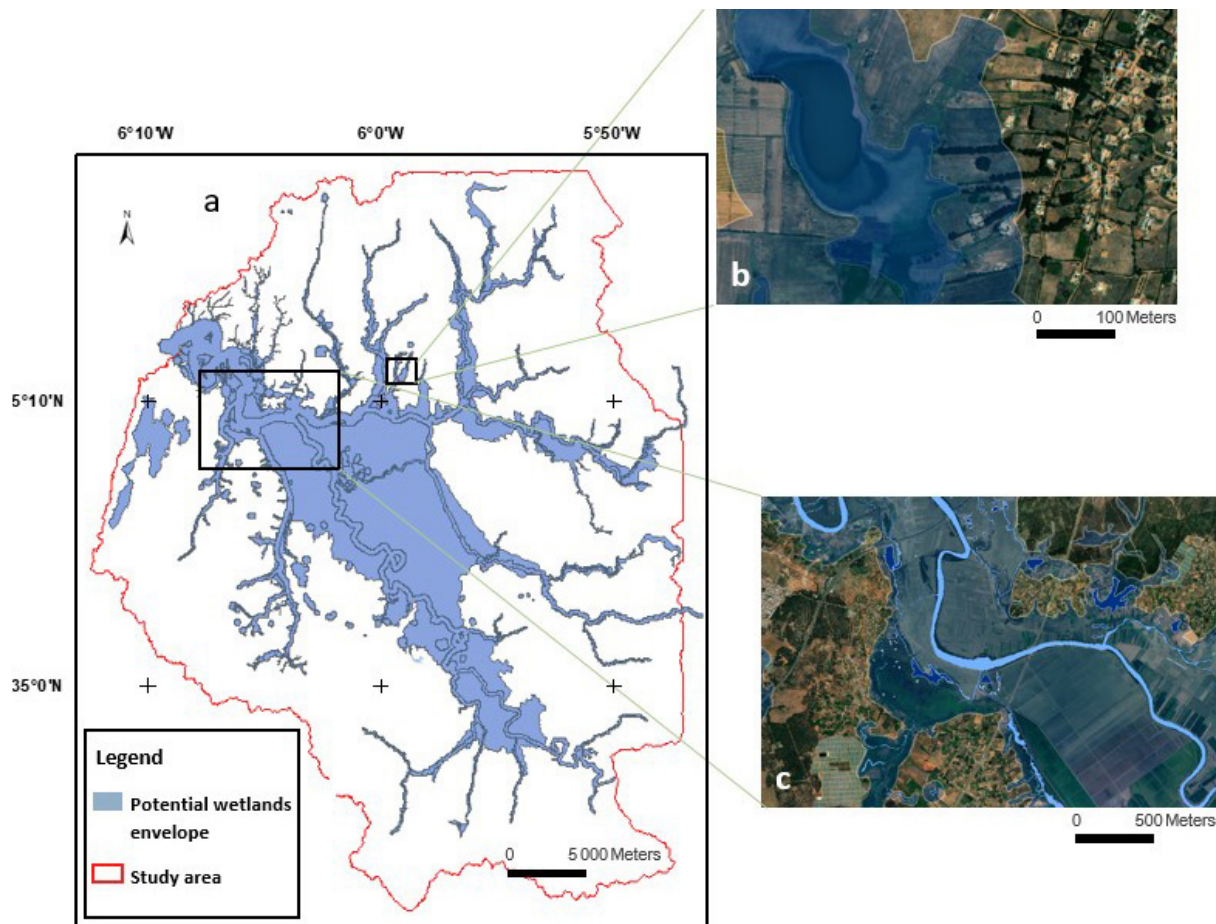
Figure 10. Map of potential wetlands areas calculated using the topographic index and buffer zone index around the hydrographic network. (a) at the scale of the Lower Loukkos sub-basin, (b) in the Bdawa Oulad Mesbah marshland and (c) on the guard dam
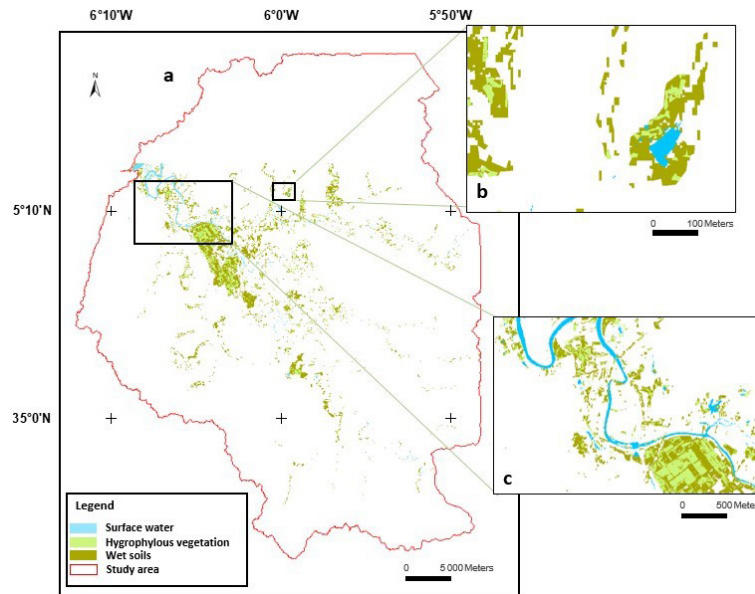
Figure 11. Envelopes of wetland-dominated areas in the Lower Loukkos Basin calculated through thresholding on the NDMI, NDVI, and MNDWI indices

bodies was estimated to be 445 hectares, classified through spectral thresholding on the mND-WI channel. The calculated area for wetland-dominated zones is 12 045 hectares.

The delimitation of existing wetlands

The delineation of EW was performed shown in Figure 12 was based on the mapping of the PW areas using a Google image with a spatial resolution of 1 meter.

Covering an area of 58.27 km², the existing wetlands (EW) comprise 33.14 km² of natural wetland areas and 25.13 km² of artificial wetlands (Adir rice fields). This represents only 6.6% of the surface area of the potential wetland zones. The natural effective wetland zones account for 92.05% of the surface area of the Lower Loukkos
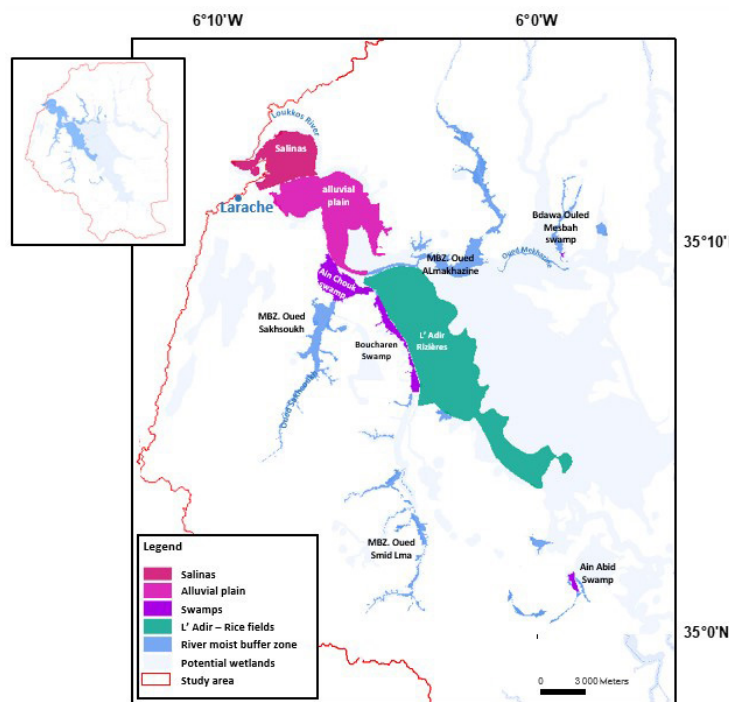
Figure 12. Model of the existing wetlands areas in the Lower Loukkos overlaying the potential wetland areas

Table 3. Confusion matrix of the model predicting the EW mapped by Computer-Assisted Photo Interpretation (CAPI) with the EW map, the pedological map, and the field surveys:

		Hydromorphic soils from soil maps		Wet soils from field samples	
		Humid	Not humid	Humid	Not humid
Existing wetlands	Humid	3.72%	0.76%	54.28%	5,49%
	Not humid	0.61%	94.91%	3.91%	36,32%
Kappa coefficient		–	83.62%	–	80.57%

Basin, as designated by the Ramsar Convention (EL AGBANI and al., 2003).

To assess the delineation of the EW after surface classification based on the wet/non-wet criterion of the PW envelope, the confusion matrices and cross-tabulations of the EW with the results from field surveys and pedological maps yielded the following Kappa indices: 0.80 and 0.83 shown in Table 3.

The Kappa index indicates a strong agreement between the results of our methodological approach and the soil data. The maps tracking the recurrent submerged areas, which recorded water land cover frequency on a monthly basis from 1984 to 2015 from the Global Surface Water Explorer provided by EC-JRC, UN-E and Google, are also consistent with the results of this study, with a Kappa value of 0.94.

The difference observed between surface area of the area of PW and EW can be attributed to several factors, including the impact of increasing temperatures on the Loukkos region in recent decades and the decrease in precipitation (Larabi and al., 2017), as well as changes in land use in the Lower Loukkos Basin. The construction of the Oued El Makhazine and Dar Khroufa dams, as well as the expansion of irrigation canals, have significantly reduced the contributions from the contributing area and the extent of wetlands. Road networks impede communication between different wetland areas, and agricultural expansion has encroached upon wetland habitats.

Method limits

From a methodological perspective, the object-oriented approach proved to be less relevant in classifying contrasting areas, such as the mosaic of the complex in the Loukkos estuary. Field observations revealed over-detections of potential wetland zones. Assigning wetland characteristics to non-wetland areas is generally due to the criteria used in modeling. The BKI and BZI indices used to predict areas of water accumulation that could form wetlands take into account the effect of topography on surface water runoff but neglect vertical circulation (infiltration and groundwater inputs). However, correcting errors of overestimation or omission through spatialization of the prolonged presence of water on the ground and vegetation provides good results with high-resolution Sentinel imagery. Spectral thresholding on the neo-channels NDVI, NDMI, and MNDWI can sometimes confuse components of wetland characteristic habitats with others that have the same spectral response, especially given the high diversity and complexity of units in the Loukkos estuary mosaic. Under-detections of this method have been observed, as wetlands with small diameters were not detected due to the spatial resolution of the DEM and Sentinel imagery, which is around 10 m.

CONCLUSIONS

The process of delineating wetland areas can face several challenges, including the large extent of wetlands and the seasonal and annual fluctuations of surface waters. The approach developed here has overcome these obstacles and has successfully mapped wetland areas covering an area of 57.5 km² in the Lower Loukkos Basin, representing only 6.6% of the calculated potentially wet areas. This delineation was based on predicting water accumulation zones based on topography and detecting the prolonged presence of water on the ground and vegetation. Open-access remote sensing data were used in the calculations, including unsupervised classification and photointerpretation under GIS. Sentinel imagery proved to be a powerful and suitable tool for this purpose. The mapped wetland models were validated by comparing them with the distribution of hydromorphic soils extracted from pedological maps and on-site soil survey, resulting in a Kappa value of 0.84. The cartographic results of this approach closely align with those identified by the Ramsar Convention and are consistent with the monitoring of submerged surfaces over the past

3.8 decades, which confirms these results with a Kappa value of 0.94.

The replication of the operational method described in this study will contribute to the establishment of a reliable wetland inventory database, providing a decision-support tool for wetland management.

REFERENCES

1. Aurousseau P., Squividant H. 1995. Rôle environnemental et identification cartographique des sols hydromorphes de bas-fonds. Cas du bassin versant de la rade de Brest. Ingénieries Eau Agriculture Territoires, 01, 75–85.

2. Bailly J.S., Puech C., Masse J. 2003. Application de l'imagerie à très haute résolution spatiale pour le suivi de l'hydromorphie du marais atlantique de Bourgneuf. Photointerprétation European Journal of Applied Remote Sensing, 1(39), 22–30.

3. Barnaud G. 1991. Fonctions et rôle des zones humides. Proceedings of the 24th hydraulics days National Congress of the Hydrotechnical Society of France, pp. 18–20.

4. Beltrame C., Perennou C., Guelmami A. 2015. Trends in land cover change in coastal wetlands around the Mediterranean Basin: Survey findings from 1975 to 2005. Méditerranée, 5, 97–111.

5. Bendjoudi H., Hubert P. 2002. Le coefficient de compacité de Gravelius: analyse critique d'un indice de forme des bassins versants. Hydrological Sciences Journal, 47(6), 921–930.

6. Beven K.J., Kirkby M.J. 1979. A Physically Based, Variable Contributing Area Model of Basin Hydrology. Hydrological Sciences Journal, 24(1), 43–69.

7. Bouzille J.B. 2014. Écologie des zones humides. Concepts, méthodes et démarches. TEC & DOC, Paris.

8. Brahmi N., Hatira A., Rabia M.C. 2010. Contribution de la télédétection et des systèmes d'information géographique à la prise en compte du risque de prolifération des Aedes dans les zones humides de Bizerte (Nord de la Tunisie). Physio-Géo, Physio-Géo, 4(-1),151–168.

9. Cazals C., Rapinel S., Frison P.L., Bonis A., Mercier G., Mallet C., Corgne S., Rudant J.P. 2016. Mapping and Characterization of Hydrological Dynamics in a Coastal Marsh Using High Temporal Resolution Sentinel-1A Images. Remote Sensing, 8(7), 570.

10. Corbane C., Lang S., Pipkins K., Alleaume S., Deshayes M., Garcia Millan V.E., Strasser T., Borre J.V., Toon S., Michael F. 2015. Remote sensing for mapping natural habitats and their conservation status – New opportunities and challenges. International Journal of Applied Earth Observation and Geoinformation, 37, 7–16.

11. Cowardin L. M., Myers V. I., 1974. Remote Sensing for Identification and Classification of Wetland Vegetation. The Journal of Wildlife Management, 38(2), 308–314.

12. Dakki M. 2002. Eléments pour un plan de gestion du complexe de zones humides du bas Loukkos. Rapport inédit, Projet Conservation des Marais de Larache : étude de faisabilité (2001–2002). Groupe de Recherche pour la Protection des Oiseaux au Maroc /Institut. Scientifique /Fondation CICONIA, 24.

13. Davranche A. 2008. Suivi de la gestion des zones humides camarguaises par télédétection en référence à leur intérêt avifaunistique. Ph.D. Thesis, Provence-I University, Aix-Marseille.

14. Du Y., Zhang Y., Ling F., Wang Q., Li W., Li X. 2016. Water Bodies' Mapping from Sentinel-2 Imagery with Modified Normalized Difference Water Index at 10-m Spatial Resolution Produced by Sharpening the SWIR Band. Remote Sensing, 8(4), 354.

15. Dusseux P. 2014. Exploitation de séries temporelles d'images satellites à haute résolution spatiale pour le suivi des prairies en milieu agricole. Ph.D. Thesis, Rennes 2 University, Upper Brittany.

16. El Agbani M.A., Dakki M., Benhoussa A., Hammada S., Bennig O. 2003. Fiche descriptive sur les zones humides Ramsar du complexe du bas Loukkos. Proceedings of 8th session of the Conference of the Contracting Parties.

17. El Hajj M., Baghdadi N., Zribi M. 2018. Estimation de l'humidité du sol par couplage d'images radar et optique. ISTE Groupe, London.

18. Ellenberg H., Weber H., Düll R., Wirth V., Werner W., Paulissen D. 1991. Ökologische Zeigerwerte von Flechten – erweiterte und aktualisierte Fassung. Herzogia, 23(2), 229–248.

19. Escadafal R., Gouinaud C., Mathieu R., Pouget M 1993. Le spectroradiomètre de terrain : un outil de la télédétection et de la pédologie. Cahier-ORSTOM, Pédologie, 28(1), 15–29.

20. Gao B.C. 1996. NDWI-A Normalized Difference Water Index for Remote Sensing of Vegetation Liquid Water from Space. Remote Sensing of Environment, 58(3), 257–266.

21. Gardner R.C., Finlayson, C. 2018. Global Wetland Outlook: State of the World's Wetlands and their Services to People. Stetson University College of Law Research Paper, 2020(5), 1–89.

22. Gilmore M.S., Wilson E.H., Barrett N., Civco D.L., Prisloe S., Hurd J.D., Chadwick C. 2008. Integrating multi-temporal spectral and structural information to map wetland vegetation in a lower Connecticut River tidal marsh. Remote Sensing of Environment, 112(11), 40–48.

23. Larbi A., El Hamidi M.J., Faouzi M., Bouaamlat I. 2017. Modeling the Impacts of Climate Change on the Aquifers in Morocco. International Journal of Water Resources and Arid Environments, 6(2), 133–142.

24. McCartney M., Acreman M.C. 2009. The wetlands handbook, Chapter 17 Wetlands and Water. Wiley-Blackwell, Chichester.

25. McFeeters S.K. 1996. The Use of the Normalized Difference Water Index (NDWI) in the Delineation of Surface Water Features. International Journal of Remote Sensing, 17(7), 1425–1432.

26. MEDDE and GIS Sol. 2013. Guide pour l'identification et la délimitation des sols de zones humides. Ministère de l'Écologie, du Développement Durable et de l'Énergie, Groupement d'Intérêt Scientifique Sol. Paris.

27. Merot P., Hubert-Moy L., Gascuel-Odoux C., Clement B., Durand P., Baudry J., Thenail C. 2006. A Method for Improving the Management of Controversial Wetland. Environmental Management 37, 258–270.

28. Otsu N. 1979. A threshold selection method from gray-level histograms. IEEE Transactions on Systems Man and Cybernetics, 9(1), 62–66.

29. Rapinel S. 2012. Contribution de la télédétection à l'évaluation des fonctions des zones humides : de l'observation à la modélisation prospective. Ph.D. Thesis, Rennes 2 University, Upper Brittany.

30. Rapinel S., Clement B., Hubert-Moy L. 2019. Cartographie des zones humides par télédétection : approche multi-scalaire pour une planification environnementale. Cybergeo: European Journal of Geography, document 885.

31. Skiner J., Zalewski S. 1995. Fonctions et Valeurs des zones humides méditerranéennes. Tour du Valat, Arles.

32. Vivone G., Alparone L., Chanussot J., Dalla Mura M.D., Garzelli A., Licciardi G.A., Restaino R., Wald L. 2015. A Critical Comparison Among Pansharpening Algorithms. IEEE Transactions on Geoscience and Remote Sensing, 53(5), 2565–2586.

33. Yarrow M.M., Salthe S.N. 2008. Ecological boundaries in the context of hierarchy theory. BioSystems journal, 92, 233–244.